Published in final edited form as:
Free Radic Biol Med. 2011 May 15; 50(10): 1252–1262. doi:10.1016/j.freeradbiomed.2011.02.031.

Caveolin-1 mediates Fas–BID signaling in hyperoxia-induced apoptosis

Meng Zhang[a,1], **Seon-Jin Lee**[a,1], **ChangHyeok An**[a], **Jin-fu Xu**[a,b], **Bharat Joshi**[c], **Ivan R. Nabi**[c], **Augustine M.K. Choi**[a], and **Yang Jin**[a,*]

[a]Division of Pulmonary and Critical Care, Department of Medicine, Brigham and Women's Hospital, Harvard Medical School, Boston, MA 02115, USA

[b]Department of Respiratory Medicine, Shanghai Pulmonary Hospital, Tongji University School of Medicine, Shanghai, China

[c]Department of Cellular and Physiological Sciences, Life Sciences Institute, University of British Columbia, Vancouver, BC V6T 1Z3, Canada

Abstract

Fas-mediated apoptosis is a crucial cellular event. Fas, the Fas-associated death domain, and caspase 8 form the death-inducing signaling complex (DISC). Activated caspase 8 mediates the extrinsic pathways and cleaves cytosolic BID. Truncated BID (tBID) translocates to the mitochondria, facilitates the release of cytochrome *c*, and activates the intrinsic pathways. However, the mechanism causing these DISC components to aggregate and form the complex remains unclear. We found that Cav-1 regulated Fas signaling and mediated the communication between extrinsic and intrinsic pathways. Shortly after hyperoxia (4 h), the colocalization and interaction of Cav-1 and Fas increased, followed by Fas multimer and DISC formation. Deletion of Cav-1 (Cav-$1^{-/-}$) disrupted DISC formation. Further, Cav-1 interacted with BID. Mutation of Cav-1 Y14 tyrosine to phenylalanine (Y14F) disrupted the hyperoxia-induced interaction between BID and Cav-1 and subsequently yielded a decreased level of tBID and resistance to hyperoxia-induced apoptosis. The reactive oxygen species (ROS) scavenger *N*-acetylcysteine decreased the Cav-1–Fas interaction. Deletion of glutathione peroxidase-2 using siRNA aggravated the BID–Cav-1 interaction and tBID formation. Taken together, these results indicate that Cav-1 regulates hyperoxia/ROS-induced apoptosis through interactions with Fas and BID, probably via Fas palmitoylation and Cav-1 Y14 phosphorylation, respectively.

Keywords

Hyperoxia; Fas; Caveolin-1; Apoptosis; Free radicals

Fas (CD95) is a well-documented mediator of apoptosis [1–4]. The induction of apoptosis requires the multimerization of Fas on the cell plasma membrane, which is often triggered

*Corresponding author. yjin@rics.bwh.harvard.edu (Y. Jin).
[1]These authors contributed equally to this work.

by Fas ligand (FasL) [1,2]. Subsequently, the Fas-associated death domain protein (FADD) binds to Fas through a series of interactions between the death domains [1–4]. In parallel, caspase 8 (FLICE) interacts with the FADD–Fas complex, leading to the activation of caspases (including caspase 3, 6, and 7), which are the effectors of common apoptotic pathways [5–10]. The caspase 8-mediated pathway is referred to as an "extrinsic apoptotic pathway." The complex of Fas, FADD, and procaspase 8 is termed the DISC (death-inducing signaling complex). Caspase 8 further cleaves a 22-kDa proapoptotic protein, BID (Bcl-2-interacting domain), resulting in a COOH-terminal component (which is a 15-kDa truncated form of BID, termed tBID) that translocates to the mitochondria and triggers the release of cytochrome *c* (Cyto *c*) [11–17]. Released Cyto *c* binds to procaspase 9 and activates caspase 9. Caspase 9 subsequently cleaves procaspase 3 and activates caspase 3 [11–17]. This BID-involved apoptotic pathway is termed an "intrinsic apoptotic pathway." As a result, BID is often viewed as a "bridge" between extrinsic and intrinsic apoptotic pathways [11–17].

Hyperoxia-induced lung epithelial cell apoptosis is a distinguishing characteristic of hyperoxia-induced acute lung injury [18–22]. Petrache et al. demonstrated the induction of apoptosis in murine macrophage cell lines in response to *in vitro* hyperoxia [23]. In another study, Mantell and Lee [24] exposed mice to hyperoxia and identified apoptosis as a prominent component of the acute inflammatory responses of the lungs. In addition, a strong correlation between the percentage of apoptotic cells and the severity of lung injury was recorded [24–27]. In general, hyperoxia activates both extrinsic and intrinsic apoptotic pathways and activates both initiator and effector caspases [28]. The extrinsic and intrinsic pathways of apoptosis both terminate at the execution phase, which is the final pathway of apoptosis. At the beginning of the execution phase, execution caspases are activated. This is followed by the execution caspases activating cytoplasmic endonucleases and proteases, which degrade nuclear material and cytoskeletal proteins, respectively [20–29]. Caspase 3, caspase 6, and caspase 7 function as effector, or executioner, caspases. The most common executioner of both the intrinsic and the extrinsic pathways of apoptosis is caspase 3 [20–29].

Caveolae (literally meaning "little caves") are flask-like invaginations of the plasma membrane, which were first described in the 1950s [30–34]. Cav-1, which is a 22-kDa scaffolding protein, is critical in the formation of the 50- to 100-nm Ω-shaped invaginated caveolae structure [30–34]. Recent emerging evidence suggests that Cav-1 plays a critical role in the regulation of a wide range of cellular processes, including the regulation of signal transduction, cell death, and survival [30–34]. Cav-1 functions as a scaffolding protein within the plasma membrane microdomains, where it interacts with signaling proteins [30–34]. Most caveolin-interacting proteins contain a caveolin-binding motif, which is located within the enzymatically active catalytic domain of these proteins. There is extensive published literature confirming that lungs express high levels of Cav-1 [35–39]. Although Cav-1 is widespread in a variety of lung cells, its exact function in lungs remains far from fully understood, particularly in acute lung injury.

Previously published work from our group has indicated that Cav-1 plays an important role in acute lung injury [40–42]. Lung epithelial cell apoptosis is a characteristic feature in

hyperoxia-induced lung injury, and we have shown in our recent studies that Cav-1 mediates hyperoxia-induced apoptosis [40–42] by regulating the level of survivin, which is a protein family member of the inhibitors of apoptosis [41]. In this study, we further delineate a novel mechanism by which Cav-1 regulates hyperoxia-induced apoptosis. We found that Cav-1 is an integral component in regulating Fas–BID pathways and facilitates both intrinsic and extrinsic apoptotic cell death in lung epithelial cells after hyperoxia.

Materials and methods

Chemicals and reagents

Cav-1 antibodies and small interfering RNAs (siRNAs) were purchased from Santa Cruz Biotechnology (Santa Cruz, CA, USA) and Cell Signaling (Danvers, MA, USA). Fas, FADD, BID, tBID antibodies, and glutathione peroxidase 2 (GPX2) siRNA were purchased from Santa Cruz Biotechnology. Catalase (CS) overexpression clones were purchased from Origene (Rockville, MD, USA). Cav-1 overexpression clones and adeno-Cav-1 were obtained from GeneCopoeia (Rockville, MD, USA) and Dr. Ferruccio Galbiati (University of Pittsburgh, Pittsburgh, PA, USA). Wild-type Cav-1 tyrosine Y14, Y14F (tyrosine to phenylalanine), and Y14D (tyrosine to aspartic acid) clones were obtained from Dr. Ivan R. Nabi (University of British Columbia, Vancouver, BC, Canada). Caspase activity kits were purchased from Calbiochem (Gibbstown, NJ, USA). All other reagents and chemicals were purchased from Sigma (St. Louis, MO, USA).

Cell culture and treatments

Human bronchial epithelial cells (Beas-2B) and primary mouse lung epithelial cells were cultured as described [42,43] and used for experiments after reaching subconfluent monolayers (usually between culture passages 7 and 17). Primary mouse alveolar epithelial cells were cultured from the lungs of wild-type C57BL/6 mice or Cav-1 null (Cav-$1^{-/-}$) mice as previously described [43]. Briefly, the mice were anesthetized, the trachea was cannulated, and the pulmonary circulation was perfused free of blood with a cold saline solution at 4 °C. After multiple whole lung lavages with a balanced saline solution, dispase (5 U/ml; Sigma) was instilled via the trachea to release type II cells. Contaminating cells bearing Fc receptors were removed by placing cells on plates coated with mouse IgG (Sigma). Then cells were plated on tissue culture dishes (Fisher Scientific, Pittsburgh, PA, USA) at 2×10^5 cells/cm^2 in Dulbecco's modified Eagle's medium (DMEM) supplemented with penicillin–streptomycin (Gibco, Grand Island, NY, USA) and 10% newborn calf serum (Sigma). Cells were cultured at 37 °C in an atmosphere of 7.5% CO_2 in air. The adherent cells were consistently >90% epithelial cells by immunofluorescent staining with anti-cytokeratin antibodies. After 2–5 days in culture, these cells underwent room air (RA) or hyperoxia exposure.

Beas-2B lung epithelial cells were purchased from the American Type Culture Collection (Manassas, VA, USA) and cultured in the defined medium, DMEM (Cambrex, East Rutherford, NJ, USA). All cells were grown in humidified incubators containing an atmosphere of 5% CO_2 and 95% air at 37 °C. Cell cultures were exposed to hyperoxia in modular exposure chambers as described [40–42], using 95% oxygen with 5% CO_2.

Animal exposures

Wild-type C57BL/6 mice or Cav-$1^{-/-}$ mice, 8–12 weeks of age, were maintained in laminar flow cages in a pathogen-free facility at the Brigham and Women's Hospital (BWH). All procedures were performed in accordance with and approved by the Council on Animal Care at the BWH and the National Research Council's *Guide for the Humane Care and Use of Laboratory Animals*. The C57BL/6 and Cav-$1^{-/-}$ mice were purchased from The Jackson Laboratory (Bar Harbor, ME, USA). The animals were exposed to room air or hyperoxia (95% O_2, 5% N_2) for the designated times.

Transfections and cell viability assays

Beas-2B cells were used for all the assays involved in transfection. Overexpression clones were transfected with lipoD293 (Signagen, Gaithersburg, MD, USA). Transiently transfected cells were incubated for an additional 24 h and exposed to hyperoxia. After 24 or 48 h, cell lysates were subjected to Western blot analysis and cell viability assays were performed.

Cell viability was determined using the CellTiter-Glo Luminescent Cell Viability Assay (Promega, Madison, WI, USA), as described previously [40,41,44]. In brief, cells (1×10^4 cells/ml) were plated onto 24-well plates in 1 ml of DMEM containing 10% fetal bovine serum until cell density was reached to 70–80% confluence. After the designated times, viable cells were determined based on quantitation of the ATP present, an indicator of metabolically active cells. The CellTiter-Glo assay generates a "glow-type" luminescent signal proportional to the amount of ATP present. The amount of ATP is directly proportional to the number of cells present in culture. In an alternative method, viable cells were stained by a crystal violet staining method. Plates were washed four times with tap water. After drying, the cells were lysed with 1% SDS solution, and dye uptake was measured at 550 nm using a 96-well plate reader. Cell viability was calculated from relative dye intensity compared with untreated samples.

Flow cytometry

We used the flow cytometry (FACS) and commercially available Annexin V–FITC Apoptosis Detection Kit Plus (Biovision, Mountain View, CA, USA) to determine apoptosis, as described [45,46]. Live cells were directly stained with annexin V–FITC and Sytox green dye. The Sytox green dye is impermeative to live cells and apoptotic cells, but stains necrotic cells with intense green fluorescence by binding to cellular nucleic acids. After a cell population was stained with annexin V–FITC and Sytox green dye in the provided binding buffer, apoptotic cells showed green fluorescence, dead cells showed a higher level of green fluorescence, and live cells showed little or no fluorescence. After staining, the cell populations were distinguished using flow cytometry with the 488-nm line of an argon-ion laser for excitation. Both annexin V–FITC and Sytox green dye emit green fluorescence that can be detected in the FL1 channel.

Fas multimerization (cross-linking) assays and immunoprecipitation

Beas-2B cells were treated with RA or hyperoxia for the designated time course. Cells were pelleted and washed twice in PBS and resuspended in 500 μl of PBS and treated with 2 mM cleavable cross-linker 3,3′-dithiobis(sulfosuccinimidyl proprionate) (Pierce, Rockford, IL, USA) for 15 min on ice, and the reaction was quenched with 10 mM ammonium acetate for 10 min. The cells were pelleted and washed twice in PBS and then lysed using 500 μl of lysis buffer (20 mM Tris, pH 7.4, 140 mM NaCl, 10% glycerol, 1% Triton X-100, and 2 mM EDTA) containing a protease inhibitor mixture (Sigma) on ice for 30 min with agitation. The lysates were then used for immunoprecipitations in the presence of an anti-Fas antibody (polyclonal; Santa Cruz Biotechnology) at 0.5–2 (antibody limiting) or 10 μg/ml (antibody excess). Immune complexes were precipitated using protein A–Sepharose (Santa Cruz Biotechnology) and washed three times. The precipitate was resuspended in RIPA buffer, boiled for 5 min, and resolved on SDS–polyacrylamide gel electrophoresis. The resolved samples were transferred onto a polyvinylidene difluoride (Millipore Corp., Billerica, MA, USA) membrane for Western blot analysis. The presence of Fas multimer was then detected using the appropriate primary monoclonal anti-Fas antibodies and secondary antibodies followed by detection using chemiluminescence (Pierce).

Lipid raft isolation

Lipid raft fractions were isolated by sucrose gradient ultracentrifugation as described, but in the absence of detergent [47]. Cells were lysed in ice-cold MBS buffer (25 mMMES, pH 6.5, 150 mM NaCl, 1 mM Na_3VO_4, and protease inhibitors). Lysates were adjusted to 4 ml of 40% sucrose by the addition 2 ml of 80% sucrose, 4 ml of 35% sucrose, 4 ml of 5% sucrose in MBS buffer. Samples were ultracentrifuged at 39,000 *g* for 18 h and fractionated into 12 subfractions. To validate the fractionation method, fractions were analyzed for organelle marker proteins by Western blotting. The transferrin receptor, a marker for noncaveolae plasma membrane, was well separated from the major caveolae fractions, indicating that noncaveolae plasma membrane did not significantly contaminate the major caveolae fractions. Caveolin-1 and GM-1, positive markers for caveolae, were detected from the caveolae fraction. We also measured Grp78, a marker for endoplasmic reticulum; cytochrome *c*, a marker for mitochondria; and Golgin-97, a marker for Golgi, which are compartmentalized to the higher density fractions.

Western blot analysis, immunocytochemistry, and immunoprecipitation

The following antibodies were used for immunoprecipitation and immunoblotting: monoclonal anti-caspase-3 (BD Transduction Laboratories, San Jose, CA, USA), mono- and polyclonal anti-caveolin (Santa Cruz Biotechnology), mono- and polyclonal anti-Fas (Santa Cruz Biotechnology), and mono- and polyclonal anti-BID (Santa Cruz Biotechnology). Western blot analysis or immunocytochemistry was performed as described previously [41]. For coimmunoprecipitation (co-IP) assay, briefly, cells were subjected to lysis in the immunoprecipitation buffer (50 mM Tris, pH 7.5, 150 mM NaCl, 1% w/w Igepal CA 630, and 0.05% w/v deoxycholate) supplemented with 0.1% w/v SDS, 0.1 mM Na_3VO_4, and protease inhibitors. The cells were sheared by brief sonication on ice and cellular debris was removed by centrifugation at 12,000 *g* for 10 min. Lysates were cleared initially by

incubation with protein A/G–Sepharose (Santa Cruz Biotechnology) for 1 h at 4 °C. Lysates were incubated with the designated specific polyclonal antibody or a preimmune rabbit IgG at a final concentration of 4 μg/ml each for 4 h at 4 °C. Protein A/G–Sepharose was then added for 4 h at 4 °C. Immune complexes were collected by centrifugation, washed eight times with 1 ml of the immunoprecipitation buffer lacking Na_3VO_4 and protease inhibitors, and disrupted by boiling in 1% SDS.

Confocal microscopy

Beas-2B or primary epithelial cells were grown on 35-mm/10-mm glass-bottom culture dishes (MatTek Corp., Ashland, MA, USA). After experimental treatments, cells cultured under standard growth conditions at 37 °C were stained for Cav-1 monoclonal antibodies (Santa Cruz Biotechnology) and Cy3 rabbit anti-mouse secondary antibodies (Molecular Probes, Eugene, OR, USA), at 1 μM, for 45 min. The cells were then washed with PBS, fixed, and permeabilized in 2% paraformaldehyde with 0.1% Triton X-100. The cells were again washed with PBS and wash buffer (0.5% bovine serum albumin, 0.15% glycine in PBS) and blocked with 10% goat serum in wash buffer. Immunostaining was performed using a polyclonal Fas or BID antibody (1:1000; Santa Cruz Biotechnology) and goat anti-rabbit Alexa 488-conjugated secondary antibodies (1:1000; Jackson ImmunoResearch Laboratories, West Grove, PA, USA). Cells were viewed with an Olympus Fluoview BX 61 confocal microscope (Olympus, Center Valley, PA, USA) and images were collected using a DC-330S cooled CCD camera (DAGE-MTI, Michigan City, IN, USA).

Statistical analysis

All values were expressed as means±SD from at least three independent experiments. Differences in measured variables between experimental and control groups were assessed using the Student *t* test (Statview II statistical package; Abacus Concepts, Berkeley, CA, USA). Statistically significant difference was accepted at $P<0.05$.

Results

Deletion of Cav-1 protects against hyperoxia-induced apoptosis in lung epithelial cells via both extrinsic and intrinsic pathways

In our previously published work, we have shown that the deletion of Cav-1 (Cav-$1^{-/-}$) protects against hyperoxia-induced cell death *via* the up-regulation of survivin [41]. This finding indicates that Cav-1 regulates caspase 3-mediated common apoptotic pathways after hyperoxia. In the current study, we first confirmed our previous observation, by using primary lung epithelial cells that were isolated from wild-type mice and Cav-$1^{-/-}$ mice. As shown in Fig. 1, we found that the deletion of Cav-1 protected primary lung epithelial cells against hyperoxia-induced cell death, which was detected using the CellTiter-Glo Luminescent Cell Viability Assay (as described under Materials and methods). Higher survival was recorded for epithelial cells that were isolated from Cav-$1^{-/-}$ mice after hyperoxia (48 h) in comparison to those isolated from wild-type mice (Fig. 1A). We used Western blot analysis to confirm that Cav-$1^{-/-}$ epithelial cells are resistant to hyperoxia-induced apoptosis, by measuring the active (cleaved) form of caspase 3 (Fig. 1B). In addition, we observed that the deletion of Cav-1 suppressed hyperoxia-induced caspase 3, 8,

and 9 activities (Fig. 1C), which represent the common, extrinsic, and intrinsic apoptotic pathways, respectively (Fig. 1C). This result indicates that, aside from the common apoptotic pathway mediated by caspase 3 [28,41], the deletion of Cav-1 confers protective functions against both extrinsic and intrinsic apoptosis after hyperoxia. To further validate our observation that Cav-1 facilitates a proapoptotic effect, we overexpressed Cav-1 in Beas-2B cells using overexpressing clones of Cav-1. As shown in Fig. 1D, the over-expression of Cav-1 resulted in a robust induction of apoptosis. However, a population of necrotic cells was also present in the vector control. This may have arisen because of the following factors: (1) the toxic effect of the transfection reagents and/or (2) difficulties in using annexin V staining/FACS analysis in adherent cells (annexin V/FACS methods are commonly used on floating cells).

Hyperoxia induces apoptosis via Fas-mediated pathways, facilitated by Cav-1 through modulating DISC formation

DISC formation has been well documented as a mediator of the extrinsic apoptotic pathways involved with caspase 8 [7–11]. In our study, hyperoxia induced caspase 8 activation (Fig. 1C); hence DISC formation after hyperoxia was determined in wild-type and Cav-$1^{-/-}$ cells using co-IP assays. As expected, we found that hyperoxia induced Fas–FADD interaction in wild-type cells (Fig. 2A). Interestingly, the deletion of Cav-1 decreased the interaction of Fas–FADD/caspase 8 after hyperoxia (Fig. 2A), which indicates the important role of Cav-1 in hyperoxia-induced DISC formation. In contrast, the overexpression of Cav-1 (by adeno-Cav-1) significantly enhanced the interaction between Fas and FADD (Fig. 2B). The release of Cyto *c* is hypothesized to occur as a consequence of tBID translocation from the cytosol to mitochondria [11–17]. Subsequently, released Cyto *c* binds to procaspase 9 and activates the intrinsic pathway of apoptosis [11–17]. For this reason, we then explored whether there is any change in cytosolic Cyto *c* in Cav-$1^{-/-}$ cells after hyperoxia. We found a higher amount of cytosolic cytochrome *c* present in wild-type cells after hyperoxia than in Cav-$1^{-/-}$ cells (Fig. 2C). Diminished cytochrome *c* release in cytosol from Cav-$1^{-/-}$ cells indicated that Cav-1 has an impact on the intrinsic apoptotic pathways after hyperoxia, in addition to its regulation of DISC formation and extrinsic apoptosis.

Cav-1 regulates the extrinsic pathway of apoptosis after hyperoxia via direct interaction with DISC components

To expand our knowledge of the mechanisms by which Cav-1-regulated hyperoxia induces the extrinsic apoptotic pathway, we investigated the colocalization and interaction between Cav-1 and Fas. We found that Cav-1 colocalized with Fas 4 h after hyperoxia (Fig. 3A). We used co-IP assays to confirm that hyperoxia induces the Cav-1–Fas interaction, by using both whole-cell lysate (Fig. 3B, left) and isolated lipid rafts (Fig. 3B, right). There was an increase in these interactions after short-term exposure to hyperoxia (4–12 h). Direct interaction between Cav-1 and caspase 8 was not found (data not shown). Furthermore, we found that prolonged hyperoxia (>24 h) eliminated the interaction between Cav-1 and Fas (Fig. 3B, left) in the absence of decreased Fas–Cav-1 protein expression (data not shown). This result suggests that prolonged hyperoxia triggers Fas trafficking and the possible dissociation from Cav-1.

Considering that Fas multimerization is required to mediate DISC formation and apoptosis [7–11], we first studied the effect of hyperoxia on Fas cross-linking and multimer formation. We assessed the Fas multimerization by immunoprecipitation (Fig. 3C), using a limited amount of anti-Fas antibodies, as described previously by Rehemtulla et al. [48]. Briefly, the principle of using a limited amount of anti-Fas antibody to detect Fas multimerization is that when the antibody is limiting, more Fas molecules are immunoprecipitated if aggregation occurs after hyperoxia. In contrast, when the antibody is in excess, equal amounts of Fas molecules should be immunoprecipitated [48]. In our study, we found that short-term exposure to hyperoxia resulted in increased Fas multimer formation (Fig. 3C) and Fas–Cav-1 interaction (Fig. 3B).

We then confirmed our observation by comparing the Fas level in the presence and absence of reducing agents, as described in previous published literature [49]. Without the addition of a reducing agent (dithiothreitol, DTT), the molecular weight of protein multimers increases compared to the monomer or oligomer of the protein under reducing conditions (with DTT). The amount of multimer formation may be determined by comparing the amount of monomer/oligomer [49]. We found that under reducing conditions, hyperoxia caused an increase in the amount of the Fas monomer (Fig. 3C, blot inset, open arrow), whereas under nonreducing conditions, hyperoxia caused a decrease in the amount of the Fas monomer (Fig. 3C, blot inset, solid arrow). This result indicates that hyperoxia induced the formation of the Fas multimer. Fas multimers retain a higher molecular weight because of the large size of the protein under nonreducing conditions. Therefore, under nonreducing conditions, an increase in Fas multimerization shows a relatively lower monomer band at the site of lower molecular weight (Fig. 3C, blot inset, solid arrow). We subsequently determined the trafficking of Fas, after multimerization. We found that prolonged hyperoxia led to Fas trafficking from lipid rafts to non-lipid rafts over a 24-h period (Fig. 3D). Lanes 2–5 (Fig. 3D) indicated the proportion of the lipid raft, which was inferred from the lipid raft marker protein flotillin-1. By using densitometry, we found that the amount of Fas protein in the lipid rafts decreased after prolonged hyperoxia (Fig. 3D, red frame), through comparison of the amount of Fas protein within lanes 2–5 (Fig. 3D). We then showed that deletion of Cav-1 interrupted the formation of the hyperoxia-induced Fas multimer (Fig.3E). To confirm that the impaired Fas multimerization is not due to a lack of Fas protein expression in Cav-$1^{-/-}$ cells, we examined the expression of the Fas protein in primary lung epithelial cells, which were isolated from wild-type and Cav-$1^{-/-}$ mice. By using Western blot analysis, we found that there is a slightly increased level of Fas protein expression in Cav-$1^{-/-}$ cells (Fig. 3F). This result further confirms that the deletion of Cav-1 disrupts Fas multimer formation, rather than decreasing the expression of the Fas protein.

Role of ROS in hyperoxia-induced Cav-1–Fas interaction

To characterize further the interaction between Cav-1 and Fas after hyperoxia, we pretreated Beas-2B cells with *N*-acetylcysteine (NAC; 30 nM), which is a reactive oxygen species (ROS) scavenger, followed by short-term (4 h) exposure to hyperoxia. We found that NAC partially eliminated the interaction of Cav-1 and Fas 4 h after hyperoxia (Fig. 4A), indicating that hyperoxia induces the Cav-1–Fas interaction at least partially via the generation of ROS (Fig. 4A). Additionally, we found that pretreatment with 2-

bromopalmitic acid (2-Br; 1 μM) significantly disrupted Cav-1–Fas interactions in Beas-2B cells after hyperoxia (Fig. 4B). Because 2-Br is known to inhibit palmitoylation [48], this result suggested that Fas interacted with Cav-1 via palmitoylation.

Direct interaction of Cav-1 with BID and facilitation of BID truncation to form tBID by caspase 8 after hyperoxia

Whereas this study has indicated the crucial role of Cav-1 in extrinsic apoptosis mediated by Fas–DISC, the elevated level of caspase 9 activity observed in the lung epithelial cells after hyperoxia requires explanation. To study the potential role of Cav-1 in the hyperoxia-induced intrinsic pathway, we first determined whether Cav-1 interacted with Bcl-2 family proteins. Bcl-2 family proteins (including BID/Bax) are known to mediate the mitochondria-regulated apoptotic pathway, namely the intrinsic pathway [8–17]. Previous reports have shown that activated caspase 8 cleaves BID and produces a 15-kDa truncated form of BID, named tBID [12–15]. tBID travels to the mitochondria and triggers the release of cytochrome *c* [12–15]. Therefore, the level of tBID is important in intrinsic apoptosis [12–15]. We used Western blot analysis to show that hyperoxia induces the formation of tBID and that the deletion of Cav-1 decreased the level of tBID (Fig. 5A). We then isolated lipid rafts and determined the distribution of BID after hyperoxia. We found that hyperoxia induced the trafficking of BID into the lipid rafts (Fig. 5B, solid black frame). We also consistently observed a time-dependent increase in the tBID protein levels in the non-lipid rafts portion (Fig. 5B, dashed red frames). Thus, we hypothesize that the trafficking of BID into rafts plays a role in hyperoxia-induced intrinsic apoptosis. Fig. 5A provides evidence that tBID formation required Cav-1. This result indicates that Cav-1 is critical in the process of hyperoxia-induced cleavage of BID by caspase 8. We then found that Cav-1 colocalized with BID and that this colocalization significantly increased after 4 h of hyperoxia (Fig. 5C). We used co-IP assays to confirm the interaction between Cav-1 and BID (Fig. 5D, top, red triangles). To study how Cav-1 interacted with BID, a mutated Cav-1 tyrosine Y14 was transfected into Beas-2B cells, with the wild-type Y14 clone being used as a control. We found that the mutation of tyrosine to phenylalanine (Y14F) abolished robustly the hyperoxia-induced interaction between Cav-1 and BID, whereas no significant difference was found when tyrosine was mutated to aspartic acid (Y14D) (Fig. 5D, top, red triangles). In addition, we used Western blot analysis to determine the level of tBID in cells transfected with wild-type Y14, Y14F, and Y14D clones after hyperoxia (Fig. 5D, bottom). As expected, we again found that the Y14F mutant (but not the Y14D) decreased the level of hyperoxia-induced tBID (Fig. 5D, bottom). This effect was more prominent after 24 h exposure of hyperoxia (Fig. 5D, bottom, red arrows). To confirm the functional role of the Cav-1–BID interaction, we measured hyperoxia-induced cell death after transfecting cells with Y14 wild-type clones, Y14D clones, and Y14F clones. We found that the transfection of Y14F protected Beas-2B cells against hyperoxia-induced cell death (Fig. 5E).

The role of ROS in hyperoxia-induced Cav-1-Fas/BID interactions

We initially determined the effect of hyperoxia on Cav-1 Y14 tyrosine phosphorylation. Considering the important roles of Cav-1 tyrosine Y14 phosphorylation indicated by this study (Fig. 5), we determined whether hyperoxia directly modulates the phosphorylation of Cav-1 Y14. Similar to our findings for ROS (H_2O_2, 90 μM, 20 min), we found that 4 h of

hyperoxia induced Cav-1 phosphorylation in primary lung epithelial cells (Fig. 6A) and that this effect may be blocked by NAC (30 nM), which is a ROS scavenger (Fig. 6B). In addition, by transfecting Beas-2B cells with GPX2 siRNA, we found that the suppression of GPX2 by siRNA augmented the interaction of Cav-1–BID and increased the formation of tBID (Fig. 6C, left). In contrast, after the overexpression of catalase in Beas-2B cells, we observed that the Cav-1–BID interaction was slightly decreased (Fig. 6C, right).

Discussion

The hyperoxia-induced Fas pathway has been reported to occur in both lung epithelial apoptosis and necrosis after hyperoxia [28,29]. However, the mechanism that triggers this hyperoxia signaling pathway in the absence of FasL remains unclear. In this study, we report that Cav-1 functions as the assembling panel for the aggregation of Fas receptors, which facilitates Fas multimerization and the truncation of BID after hyperoxia. Hence, Cav-1 is crucial for cells to form DISC after hyperoxia. We also report the novel finding that Cav-1 triggers the initial steps of apoptotic cascade after hyperoxia, followed by the facilitation of extrinsic and intrinsic apoptosis. Thus, the current study provides an improved explanation for the proapoptotic effect of Cav-1 in the model of hyperoxia-induced lung epithelial cell apoptosis. After examining the human Fas protein sequence, we indeed identified a potential Cav-1 binding motif, "GL**H**HDGQ**F**C**H**," starting at amino acid 53. Presumably, the antagonism of this binding motif may potentially result in disruption of the Fas–Cav-1 interaction and Fas multimerization after hyperoxia. Hence, future therapeutic agents targeted toward inhibiting the Fas–Cav-1 interaction may be developed to treat acute lung injury.

Another original finding delineated by this study is the mechanism by which Cav-1 regulates communication between the extrinsic and the intrinsic apoptotic pathways that are induced by hyperoxia. In our previous publications we showed that Cav-1 increased the activity of caspase 3 after hyperoxia [41]. Caspase 3 mediates the common apoptotic pathway in hyperoxia-induced apoptosis [28]. We found that the deletion of Cav-1 (Cav-$1^{-/-}$) also decreased the activities of hyperoxia-induced caspases 8 and 9 (Fig. 1), which represent the extrinsic and intrinsic apoptotic pathways, respectively [10–17]. Therefore, we suspected that Cav-1 is involved in both extrinsic and intrinsic pathways after hyperoxia. Our results from the BID mutants–Cav-1 interaction and tBID formation indicate that side-chain polarity plays an important role in Cav-1 conformation, which subsequently affects the Cav-1–BID interaction. Our results are consistent with previous observations that Cav-1 tyrosine phosphorylation is required for Cav-1 to interact with other signal proteins, such as CD26 and members of the Ras signaling pathway [50,51].

We have shown that the binding of Cav-1 with DISC components (i.e., Fas and FADD) is probably accomplished *via* palmitoylation (Fig. 4). Previous studies have also shown that Fas multimerization is accomplished via palmitoylation [47]. At the COOH component of Cav-1, there are three cysteine palmitoylation sites (Cys 133, 143, and 156), which may be crucial for Fas–Cav-1 interactions after hyperoxia. Furthermore, the reversibility of the palmitoylation process may explain the interaction–dissociation cycle of Fas–Cav-1 after prolonged hyperoxia, which is also a reversible process. Basically, the Fas complex

dissociates from Cav-1 and is trafficked away from the lipid rafts (Fig. 3), which is probably an internalized process [48–52]. Therefore, the palmitoylation between Cav-1 and Fas should occur near the COOH-terminus. Thus, the DISC that includes caspase 8 is probably positioned adjacent to the Cav-1 COOH-terminus. The physical interaction between Cav-1 and BID occurs close to the N-terminus at tyrosine Y14 and is a crucial step that increases the physical proximity of BID to caspase 8 for cleavage (Fig. 7).

In our study, we also showed that hyperoxia increased the phosphorylation of Y14 (Fig. 6). This result is consistent with a previous report that ROS augment the phosphorylation of Y14 [52,53]. Cav-1 tyrosine Y14 is considered the principal site for recognition by c-Src kinase [54]. Lee et al. [55] also provided evidence that tyrosine-kinase signaling is regulated by tyrosine-phosphorylated Cav-1. Jiang et al. [56] suggested that the phosphorylation of Cav-1 at the tyrosine Y14 terminus after bromocriptine treatment may contribute to the sensitization of apoptosis in GH3 cells that have been exposed to bromocriptine. In the same year, Shajahan et al. [57] showed that the Src phosphorylation of Tyr 14 on Cav-1 regulates paclitaxel-mediated apoptosis in MCF-7 breast cancer cells. Phosphorylated Cav-1 was shown to trigger apoptosis by increasing mitochondrial permeability more efficiently than nonphosphorylated Cav-1 [58]. However, the authors of these studies did not explore the mechanism by which phosphorylated Cav-1 increased apoptosis. Similar to what is shown in our model of hyperoxia-induced apoptosis, we hypothesize that phosphorylated Cav-1 is crucial for anchoring BID and active caspase 8 together at a docking site, which then facilitates the cleavage to tBID *via* active caspase 8. Thus, tBID may increase mitochondrial permeability and the release of Cyto *c*. Based on our functional data of cell death after hyperoxia (Fig. 5), we conclude that Cav-1 may serve as an assembling panel on which the pTyr-binding molecules (in this case, BID) may physically interact with caspase 8. Therefore, our results indicate that the truncation of BID by caspase 8 is an anchorage-dependent process.

In addition, we showed that ROS mediated hyperoxia-induced Fas–Cav-1 and Cav-1–BID interactions (Figs. 4 and 6). Our study provides the first documentation that the Cav-1–BID interaction and BID truncation may be manipulated by ROS *via* the regulation of Cav-1 Y14 phosphorylation. However, the effect of ROS on the modification of Fas is more complicated. Previous publications have demonstrated that ROS increases the ligation of Fas [59], which is redox-regulated under physiological conditions. Redox-mediated Fas modification promotes the aggregation of Fas and its recruitment into lipid rafts, which enhances the binding of FasL [59]. The initial activation of caspase 8 causes the degradation of glutaredoxins and leads to the S-glutathionylation of Fas at the cysteine 294 terminus. This action enhances the accumulation and aggregation of Fas in lipid rafts and then the DISC assembly, which further propagates apoptosis. In our study, neither the overexpression of catalase nor the deletion of GPX2 provided consistent results with respect to the Cav-1–Fas interaction. We hypothesize that this outcome may be due to the inconsistent modification of Fas by ROS and/or the effect of ROS on Cav-1 regulation itself. Rungtabnapa et al. [60] reported that the downregulation of Cav-1 was inhibited by hydrogen peroxide preventing the formation of the Cav-1–ubiquitin complex [60]. In contrast, catalase and *N*-acetylcysteine promoted the ubiquitin and proteasomal degradation

of Cav-1. We hypothesize that ROS-regulated Cav-1–Fas interaction is a complex process, involving the modification of Fas and the prolongation of the Cav-1 half-life. The balance of all of the factors involved in the response to hyperoxia determines whether the apoptosis cascade is triggered.

In conclusion, the data obtained in this study indicate that Cav-1 mediates hyperoxia-induced lung epithelial cell apoptosis *via* Fas-mediated pathways, which subsequently trigger both intrinsic and extrinsic apoptosis. Furthermore, ROS-regulated phosphorylation of Cav-1 also plays a fundamental role in the communication between the extrinsic and the intrinsic pathways.

Acknowledgments

This work was supported by ATS Unrestricted Research Grant 2009–2010.

Abbreviations

Cav-1	caveolin-1
FADD	Fas-associated death domain protein
NAC	*N*-acetylcysteine
DISC	death-inducing signaling complex
2-Br	2-bromopalmitic acid
CS	catalase
GPX2	glutathione peroxidase 2

References

1. Ashkenazi A, Dixit VM. Death receptors: signaling and modulation. Science. 1998; 281:305–1308.
2. Takahashi T, Tanaka M, Inazawa J, Abe T, Suda T, Nagata S. Human Fas ligand: gene structure, chromosomal location and species specificity. Int. Immunol. 1994; 6:1567–1574. [PubMed: 7826947]
3. Ogasawara J, et al. Lethal effect of the anti-Fas antibody in mice. Nature. 1993; 364:806–809. [PubMed: 7689176]
4. Jones RA, et al. Fas-mediated apoptosis in mouse hepatocytes involves the processing and activation of caspases. Hepatology. 1998; 27:1632–1642. [PubMed: 9620337]
5. Algeciras-Schimnich A, Shen L, Barnhart BC, Murmann AE, Burkhardt JK, Peter ME. Molecular ordering of the initial signaling events of CD95. Mol. Cell. Biol. 2002; 22:207–220. [PubMed: 11739735]
6. Weinmann M, Jendrossek V, Handrick R, Güner D, Goecke B, Belka C. Molecular ordering of hypoxia-induced apoptosis: critical involvement of the mitochondrial death pathway in a FADD/caspase-8 independent manner. Oncogene. 2004; 23:3757–3769. [PubMed: 15034549]
7. Chatfield K, Eastman A. Inhibitors of protein phosphatases 1 and 2A differentially prevent intrinsic and extrinsic apoptosis pathways. Biochem. Biophys. Res. Commun. 2004; 323:1313–1320. [PubMed: 15451440]
8. Marconi A, Atzei P, Panza C, Fila C, Tiberio R, Truzzi F, Wachter T, Leverkus M, Pincelli C. FLICE/caspase-8 activation triggers anoikis induced by beta1-integrin blockade in human keratinocytes. J. Cell Sci. 2004; 117(Pt 24):5815–5823. [PubMed: 15507484]

9. Lombard C, Nagarkatti M, Nagarkatti PS. Targeting cannabinoid receptors to treat leukemia: role of cross-talk between extrinsic and intrinsic pathways in Delta9-tetrahydrocannabinol (THC)-induced apoptosis of Jurkat cells. Leuk. Res. 2005; 29:915–922. [PubMed: 15978942]
10. Gross A, McDonnell JM, Korsmeyer SJ. BCL-2 family members and the mitochondria in apoptosis. Genes Dev. 1999; 13:1899–1911. [PubMed: 10444588]
11. Yin XM, Oltvai ZN, Korsmeyer SJ. BH1 and BH2 domains of Bcl-2 are required for inhibition of apoptosis and heterodimerization with Bax. Nature. 1994; 369:321–323. [PubMed: 8183370]
12. Wang K, et al. BID: a novel BH3 domain-only death agonist. Genes Dev. 1996; 10:2859–2869. [PubMed: 8918887]
13. Li H, et al. Cleavage of BID by caspase 8 mediates the mitochondrial damage in the Fas pathway of apoptosis. Cell. 1998; 94:491–501. [PubMed: 9727492]
14. Luo X, et al. Bid, a Bcl2 interacting protein, mediates cytochrome c release from mitochondria in response to activation of cell surface death receptors. Cell. 1998; 94:481–490. [PubMed: 9727491]
15. Gross A, et al. Caspase cleaved Bid targets mitochondria and is required for cytochrome c release, while Bcl-xL prevents this release but not tumor necrosis factor-R1/Fas death. J. Biol. Chem. 1999; 274:1156–1163. [PubMed: 9873064]
16. Lacronique V, et al. Bcl-2 protects from lethal hepatic apoptosis induced by an anti-Fas antibody in mice. Nat. Med. 1996; 2:80–86. [PubMed: 8564847]
17. Yin XM, et al. Bid-deficient mice are resistant to Fas-induced hepatocellular apoptosis. Nature. 1999; 400:886. [PubMed: 10476969]
18. Ashbaugh DG, Bigelow DB, Petty TL. Acute respiratory distress in adults. Lancet. 1967; 2:319–323. [PubMed: 4143721]
19. Bernard GR. Acute respiratory distress syndrome: a historical perspective. Am. J. Respir. Crit. Care Med. 2005; 172:798–806. [PubMed: 16020801]
20. Rubenfeld GD, Caldwell E, Peabody E. Incidence and outcomes of acute lung injury. N. Engl. J. Med. 2005; 353:1685–1693. [PubMed: 16236739]
21. Matute-Bello G, Frevert CW, Martin TR. Animal models of acute lung injury. Am. J. Physiol. Lung Cell. Mol. Physiol. 2008; 295:L379–L399. [PubMed: 18621912]
22. Lee PJ, Alam J, Sylvester SL, Inamdar N, Otterbein L, Choi AM. Regulation of heme oxygenase-1 expression in vivo and in vitro in hyperoxic lung injury. Am. J. Respir. Cell Mol. Biol. 1996; 14:556–568. [PubMed: 8652184]
23. Petrache I, Choi ME, Otterbein LE, Chin BY, Mantell LL, Horowitz S, Choi AM. Mitogen-activated protein kinase pathway mediates hyperoxia-induced apoptosis in cultured macrophage cells. Am. J. Physiol. 1999; 277(3 Pt 1):L589–L595. [PubMed: 10484467]
24. Mantell LL, Lee PJ. Signal transduction pathways in hyperoxia-induced lung cell death. Mol. Genet. Metab. 2000; 71:359–370. [PubMed: 11001828]
25. Zaher TE, Miller EJ, Morrow DM, Javdan M, Mantell LL. Hyperoxia-induced signal transduction pathways in pulmonary epithelial cells. Free Radic. Biol. Med. 2007; 42:897–908. [PubMed: 17349918]
26. Buckley S, Barsky L, Driscoll B, Weinberg K, Anderson KD, Warburton D. Apoptosis and DNA damage in type 2 alveolar epithelial cells cultured from hyperoxic rats. Am. J. Physiol. 1998; 274(5 Pt 1):L714–L720. [PubMed: 9612286]
27. Pagano A, Barazzone-Argiroffo C. Alveolar cell death in hyperoxia-induced lung injury. Ann. N. Y. Acad. Sci. 2003; 1010:405–416. [PubMed: 15033761]
28. Wang X, Wang Y, Kim HP, Nakahira K, Ryter SW, Choi AM. Carbon monoxide protects against hyperoxia-induced endothelial cell apoptosis by inhibiting reactive oxygen species formation. J. Biol. Chem. 2007; 282:1718–1726. [PubMed: 17135272]
29. Tang PS, Mura M, Seth R, Liu M. Acute lung injury and cell death: how many ways can cells die? Am. J. Physiol. Lung Cell. Mol. Physiol. 2008; 294:L632–L641. [PubMed: 18203816]
30. Yamada E. The fine structure of the gall bladder epithelium of the mouse. J. Biophys. Biochem. Cytol. 1955; 1:445–458. [PubMed: 13263332]
31. Palade GE. Fine structure of blood capillaries. J. Appl. Phys. 1953; 24:1424.

32. Rothberg KG, Heuser JE, Donzell WC, Ying YS, Glenney JR, Anderson RG. Caveolin, a protein component of caveolae membrane coats. Cell. 1992; 68:673–682. [PubMed: 1739974]
33. Schwab W, Galbiati F, Volonte D, Hempel U, Wenzel KW, Funk RH, Lisanti MP, Kasper M. Characterisation of caveolins from cartilage: expression of caveolin-1, −2 −3 in chondrocytes in alginate cell culture of the rat tibia. Histochem. Cell Biol. 1999; 112:41–49. [PubMed: 10461811]
34. Fujimoto T, Kogo H, Nomura R, Une T. Isoforms of caveolin-1 and caveolar structure. J. Cell Sci. 2000; 113(Pt 19):3509–3517. [PubMed: 10984441]
35. Glenney JR Jr, Soppet D. Sequence and expression of caveolin, a protein component of caveolae plasma membrane domains phosphorylated on tyrosine in Rous sarcoma virus-transformed fibroblasts. Proc. Natl. Acad. Sci. U. S. A. 1992; 89:10517–10521. [PubMed: 1279683]
36. Scherer PE, Tang Z, Chun M, Sargiacomo M, Lodish HF, Lisanti MP. Caveolin isoforms differ in their N-terminal protein sequence and subcellular distribution: identification and epitope mapping of an isoform-specific monoclonal antibody probe. J. Biol. Chem. 1995; 270:16395–16401. [PubMed: 7608210]
37. Fang PK, Solomon KR, Zhuang L, Qi M, McKee M, Freeman MR, Yelick PC. Caveolin-1alpha and −1beta perform nonredundant roles in early vertebrate development. Am. J. Pathol. 2006; 169:2209–2222. [PubMed: 17148682]
38. Thomas CM, Smart EJ. Caveolae structure and function. J. Cell. Mol. Med. 2008; 12:796–809. [PubMed: 18315571]
39. Han JM, Kim Y, Lee JS, Lee CS, Lee BD, Ohba M, Kuroki T, Suh PG, Ryu SH. Localization of phospholipase D1 to caveolin-enriched membrane via palmitoylation: implications for epidermal growth factor signaling. Mol. Biol. Cell. 2002; 13:3976–3988. [PubMed: 12429840]
40. Jin Y, Kim HP, Chi M, Ifedigbo E, Ryter SW, Choi AM. Deletion of caveolin-1 protects against oxidative lung injury via up-regulation of heme oxygenase-1. Am. J. Respir. Cell Mol. Biol. 2008; 39:171–179. [PubMed: 18323531]
41. Zhang M, Lin L, Lee SJ, Mo L, Cao J, Ifedigbo E, Jin Y. Deletion of caveolin-1 protects hyperoxia-induced apoptosis via survivin-mediated pathways. Am. J. Physiol. Lung Cell. Mol. Physiol. 2009; 297:L945–L953. [PubMed: 19767411]
42. Jin Y, Kim HP, Cao J, Zhang M, Ifedigbo E, Choi AM. Caveolin-1 regulates the secretion and cytoprotection of Cyr61 in hyperoxic cell death. FASEB J. 2009; 23:341–350. [PubMed: 18801924]
43. O'Brien AD, Standiford TJ, Bucknell KA, Wilcoxen SE, Paine R III. Role of alveolar epithelial cell intercellular adhesion molecule-1 in host defense against Klebsiella pneumoniae. Am. J. Physiol. 1999; 276(6 Pt 1):L961–L970. [PubMed: 10362721]
44. Ochel HJ. Correlation between crystal violet dissolution assay and manual colony counting on the in vitro effects of Hsp90-inhibitors. J. Exp. Ther. Oncol. 2005; 5:9–13. [PubMed: 16416596]
45. Kim YM, Talanian RV, Billiar TR. Nitric oxide inhibits apoptosis by preventing increases in caspase-3-like activity via two distinct mechanisms. J. Biol. Chem. 1997; 272:31138–31148. [PubMed: 9388267]
46. Gogal RM Jr, Smith BJ, Kalnitsky J, Holladay SD. Analysis of apoptosis of lymphoid cells in fish exposed to immunotoxic compounds. Cytometry. 2000; 39:310–318. [PubMed: 10738285]
47. Kim HP, Wang X, Galbiati F, Ryter SW, Choi AM. Caveolae compartmentalization of heme oxygenase-1 in endothelial cells. FASEB J. 2004; 18:1080–1099. [PubMed: 15226268]
48. Rehemtulla A, Hamilton CA, Chinnaiyan AM, Dixit VM. Ultraviolet radiation-induced apoptosis is mediated by activation of CD-95 (Fas/APO-1). J. Biol. Chem. 1997; 272:25783–25786. [PubMed: 9325306]
49. Oury TD, Crapo JD, Valnickova Z, Enghild JJ. Human extracellular superoxide dismutase is a tetramer composed of two disulphide-linked dimers: a simplified, high-yield purification of extracellular superoxide dismutase. Biochem. J. 1996; 317:51–57. [PubMed: 8694786]
50. Paige LA, Nadler MJ, Harrison ML, Cassady JM, Geahlen RL. Reversible palmitoylation of the protein-tyrosine kinase p56lck. J. Biol. Chem. 1993; 268:8669–8674. [PubMed: 8473310]
51. Ohnuma K, Yamochi T, Uchiyama M, Nishibashi K, Iwata S, Hosono O, Kawasaki H, Tanaka H, Dang NH, Morimoto C. CD26 mediates dissociation of Tollip and IRAK-1 from caveolin-1 and

induces upregulation of CD86 on antigen-presenting cells. Mol. Cell. Biol. 2005; 25:7743–7757. [PubMed: 16107720]

52. Sasai K, Kakumoto K, Hanafusa H, Akagi T. The Ras–MAPK pathway downregulates caveolin-1 in rodent fibroblast but not in human fibroblasts: implications in the resistance to oncogene-mediated transformation. Oncogene. 2007; 26:449–455. [PubMed: 16832346]
53. Sun Y, Hu G, Zhang X, Minshall RD. Phosphorylation of caveolin-1 regulates oxidant-induced pulmonary vascular permeability via paracellular and transcellular pathways. Circ. Res. 2009; 105:676–685. (15 p following 685). [PubMed: 19713536]
54. Khanna S, Roy S, Park HA, Sen CK. Regulation of c-Src activity in glutamate-induced neurodegeneration. J. Biol. Chem. 2007; 282:23482–23490. [PubMed: 17569670]
55. Lee H, Volonte D, Galbiati F, Iyengar P, Lublin DM, Bregman DB, Wilson MT, Campos-Gonzalez R, Bouzahzah B, Pestell RG, Scherer PE, Lisanti MP. Constitutive and growth factor-regulated phosphorylation of caveolin-1 occurs at the same site (Tyr-14) in vivo: identification of a c-Src/Cav-1/Grb7 signaling cassette. Mol. Endocrinol. 2000; 14:1750–1775. [PubMed: 11075810]
56. Jiang YN, Li YH, Ke MW, Tseng TY, Tang YB, Huang MC, Cheng WT, Ju YT. Caveolin-1 sensitizes rat pituitary adenoma GH3 cells to bromocriptine induced apoptosis. Cancer Cell Int. 2007; 7:1. [PubMed: 17331262]
57. Shajahan AN, Wang A, Decker M, Minshall RD, Liu MC, Clarke R. Caveolin-1 tyrosine phosphorylation enhances paclitaxel-mediated cytotoxicity. J. Biol. Chem. 2007; 282:5934–5943. [PubMed: 17190831]
58. Shajahan AN, Wang A, Decker M, Minshall RD, Liu MC, Clarke R. Caveolin-1 tyrosine phosphorylation enhances paclitaxel-mediated cytotoxicity. J. Biol. Chem. 2007; 282:5934–5943. [PubMed: 17190831]
59. Anathy V, Aesif SW, Guala AS, Havermans M, Reynaert NL, Ho YS, Budd RC, Janssen-Heininger YM. Redox amplification of apoptosis by caspase-dependent cleavage of glutaredoxin 1 and S-glutathionylation of Fas. J. Cell Biol. 2009; 184:241–252. [PubMed: 19171757]
60. Rungtabnapa P, Nimmannit U, Halim H, Rojanasakul Y, Chanvorachote P. Hydrogen peroxide inhibits non-small cell lung cancer cell anoikis through the inhibition of caveolin-1 degradation. Am. J. Physiol. Cell Physiol. 2011; 300:C235–C245. [PubMed: 21148404]

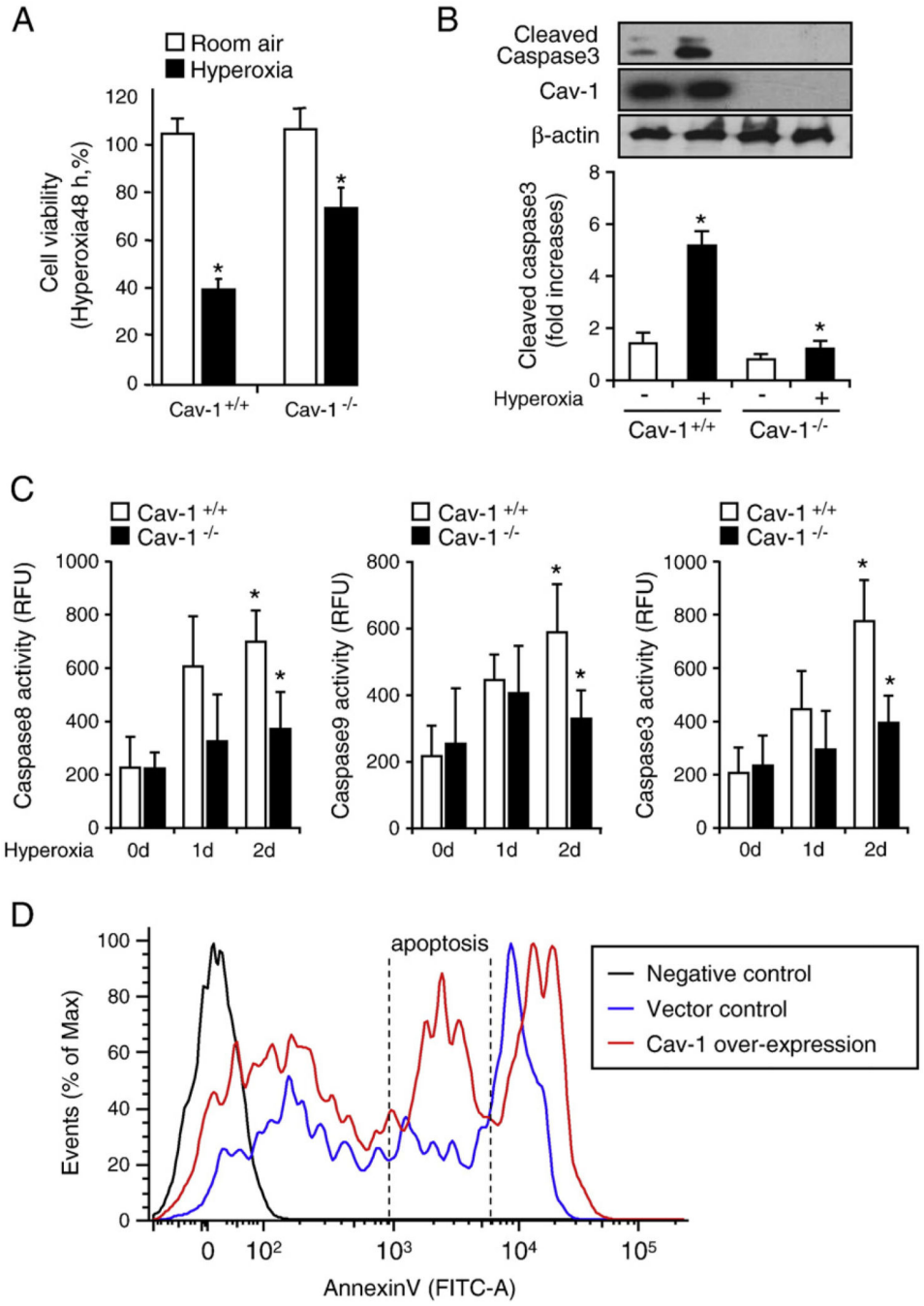

Fig. 1.

Deletion of Cav-1 protected lung epithelial cells against hyperoxia-induced apoptosis *via* the regulation of apoptotic pathways. Primary mouse lung epithelial cells were used in these experiments. Cells were exposed to room air (i.e., 20.8% oxygen + 78.08% nitrogen) or hyperoxia (95% oxygen + 5% balanced nitrogen) conditions. At designated times (i.e., after 4, 24, and 48 h), cells were collected and subjected to cell survival assays, namely, Western blot analysis or caspase activity assay. (A) The deletion of Cav-1 protected the primary mouse lung epithelial cells from hyperoxia-induced cell death. Primary mouse lung

epithelial cells were isolated from either wild-type C57BL/6 mice (Cav-$1^{+/+}$) or Cav-$1^{-/-}$ mice. The cells were then exposed to room air or hyperoxia conditions. After 48 h, cell viability was determined, as described under Materials and methods. (B) The deletion of Cav-1 protected the primary mouse lung epithelial cells against hyperoxia-induced activation of caspase 3. The epithelial cells were isolated from either wild-type C57BL/6 mice or Cav-$1^{-/-}$ mice. The cells were then exposed to hyperoxia conditions (48 h), after which cell lysates were obtained and subjected to Western blot analysis. (C) The deletion of Cav-1 protected the primary mouse lung epithelial cells against hyperoxia-induced caspase 3, 8, and 9 activation. Cells were exposed to room air, 24 h hyperoxia, or 48 h hyperoxia conditions. After exposure, cell lysates were obtained and caspase activities were measured using assays as described previously [40,41]. (D) To confirm the proapoptotic effect of Cav-1, we overexpressed Cav-1 or empty vectors in Beas-2B cells. Cell death was analyzed using FACS. Live cells were directly stained with annexin V–FITC and Sytox green dye. The Sytox green dye is impermeative to live cells and apoptotic cells, but stains necrotic cells with intense green fluorescence. After staining, apoptotic cells show green fluorescence, whereas dead cells show a higher level of green fluorescence and live cells show little or much lower levels of fluorescence. Three cell populations were observed, including (1) live cells, (2) apoptotic cells, and (3) necrotic cells. All experiments presented were repeated using three independent assays with similar results. *$P<0.05$.

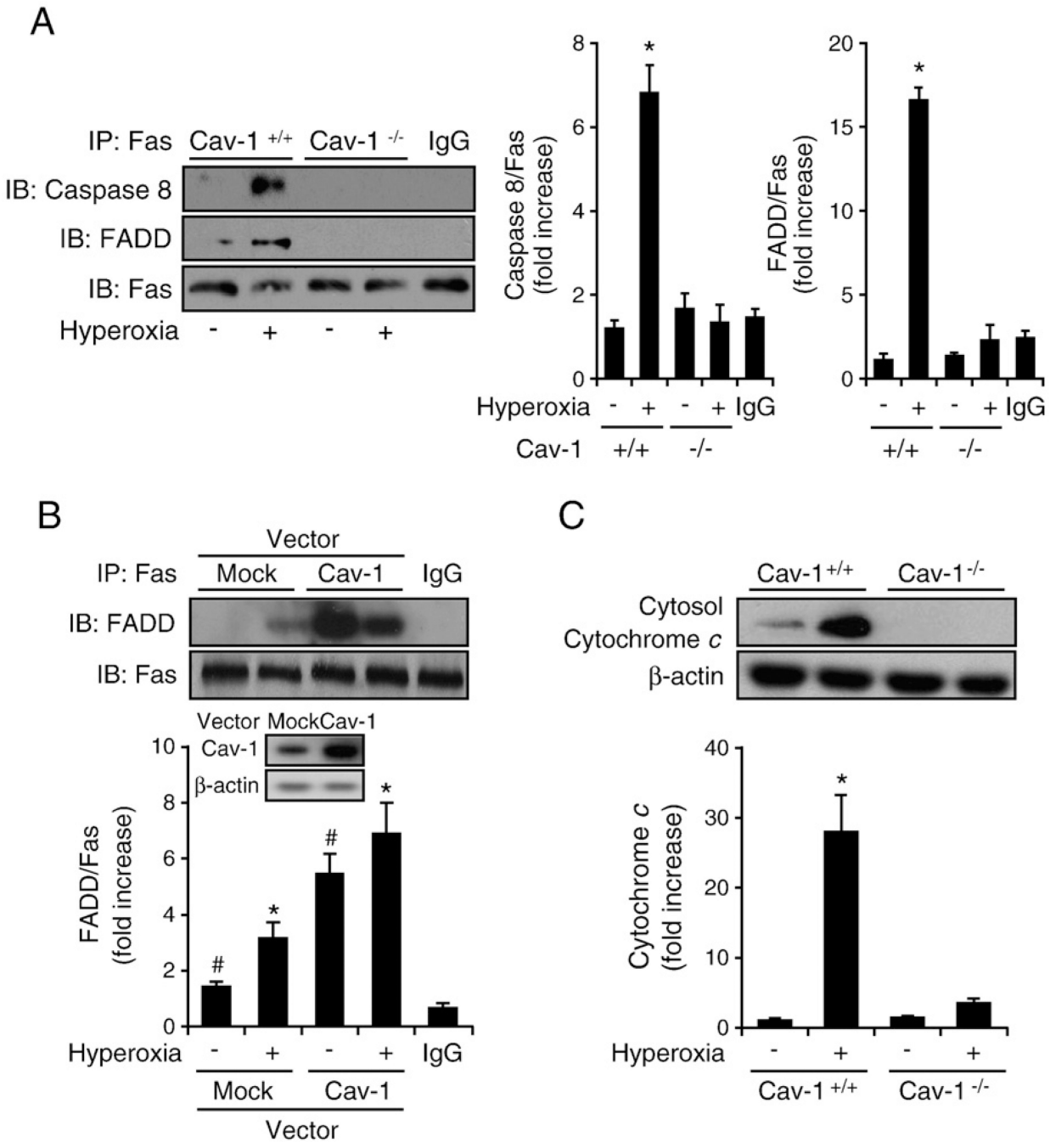

Fig. 2.

Cav-1 facilitated the hyperoxia-induced Fas–FADD/caspase 8 interaction in the absence of the Fas ligand. Primary mouse lung epithelial cells and Beas-2B human epithelial cells were used in these experiments. Cells were exposed to room air (i.e., 20.8% oxygen + 78.08% nitrogen) or hyperoxia (95% oxygen + 5% balanced nitrogen) conditions. At designated times (i.e., after 4, 24, or 48 h), the cells were collected and subjected to co-IP assay or Western blot analysis. DISC formation was determined by detecting the interaction of Fas–FADD/caspase 8. (A) The deletion of Cav-1 disrupted hyperoxia-induced DISC formation.

Primary mouse lung epithelial cells from either wild-type C57BL/6 mice (Cav-$1^{+/+}$) or Cav-$1^{-/-}$ mice were exposed to room air or hyperoxia (4 h) conditions. Co-IP assays between Fas and FADD and Fas and caspase 8 were performed as described previously. (B) Overexpressing Cav-1 facilitated Fas–FADD interaction after hyperoxia. Beas-2B cells were used in these experiments and infected with adeno-lacZ (control) and adeno-Cav-1, as described previously [41]. Cells were then exposed to hyperoxia (4 h), and co-IP assays were performed between Fas and FADD. (C) Deletion of Cav-1 prevented the release of cytochrome *c* after hyperoxia. Primary mouse lung epithelial cells from either wild-type C57BL/6 mice or Cav-$1^{-/-}$ mice were exposed to hyperoxia. After 24 h, the level of cytosol cytochrome *c* was determined by Western blot analysis, as described previously [28]. All experiments presented were repeated using three independent assays with similar results. $^{*}P<0.05$, $^{\#}P<0.01$.

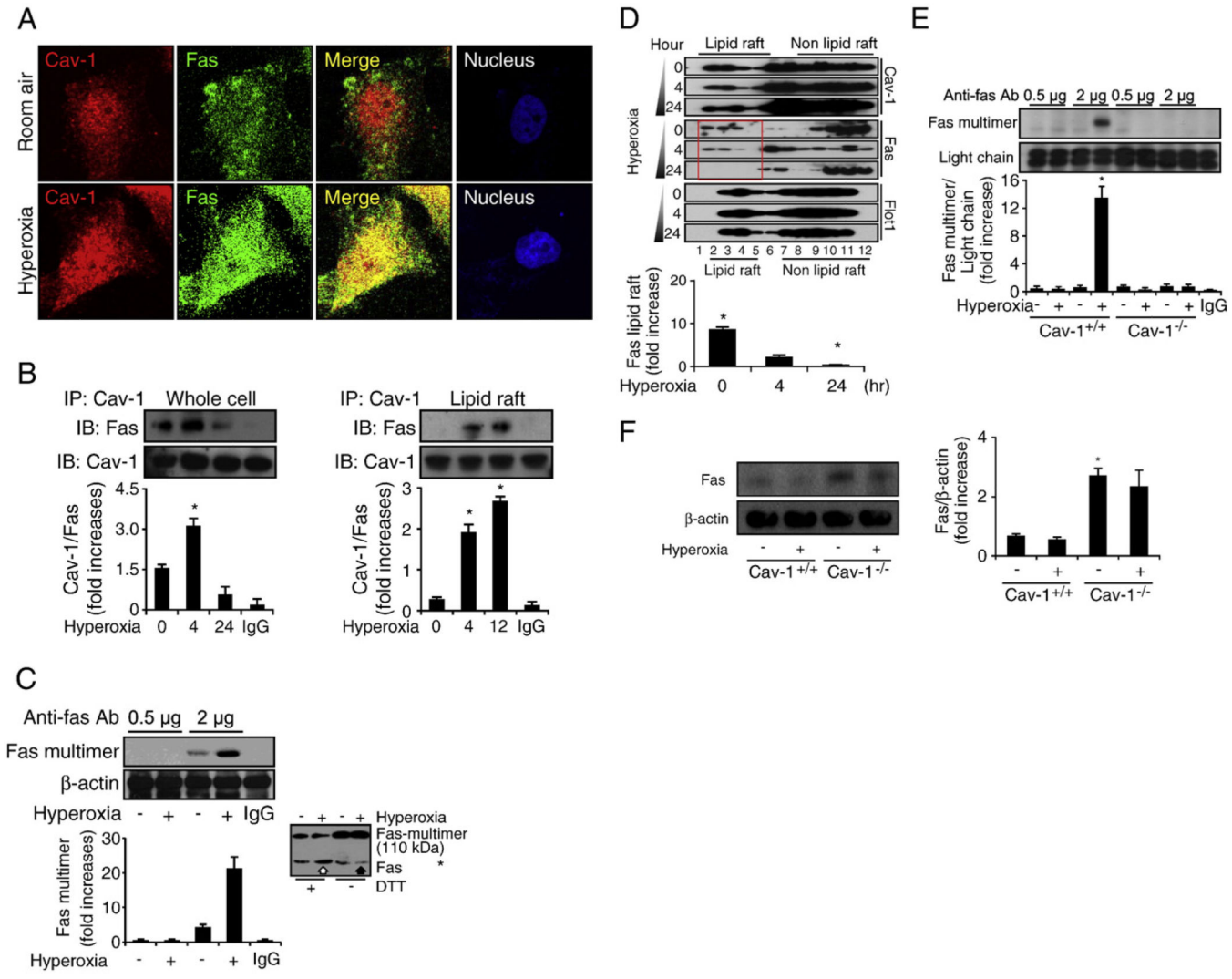

Fig. 3.

Cav-1 directly interacts with Fas and facilitates Fas–Fas multimerization after hyperoxia. Primary mouse lung epithelial cells and Beas-2B cells were used in these experiments and treated with RA or hyperoxia conditions for the designated times. (A) The colocalization between Cav-1 and Fas after hyperoxia (4 h). Beas-2B cells were exposed to RA or hyperoxia, as described previously. After 4 h, the cells were stained with anti-Fas, anti-Cav-1, and DAPI and then subjected to confocal microscopy. (B) Cav-1–Fas interaction was determined by co-IP assays. Beas-2B cells were exposed to RA or hyperoxia conditions, as indicated. On the left, whole-cell lysate was used in the co-IP assays. On the right, isolated lipid rafts were used to perform co-IP. Reverse co-IP was performed with similar results (i.e., IP, Fas; IB, Cav-1). (C) Hyperoxia-induced Fas–Fas multimerization in Beas-2B cells. Cells were exposed to hyperoxia (4 h), followed by Fas multimerization assays, as described previously [47]. Briefly, a limited amount of rabbit polyclonal anti-Fas antibody was used to precipitate Fas multimer. After fractioning by SDS–PAGE, mouse monoclonal anti-Fas antibody was used as the primary antibody to detect the precipitated Fas multimer. Using a limited amount of antibodies (0.5–2 μg), a visible difference was observed for the amount of

precipitated Fas multimers between RA-treated and hyperoxia-treated cells. When an excess amount of antibodies (15–20 μg) was used to precipitate the Fas multimer, there was no significant difference between any of the groups (not shown). (D) Hyperoxia induced Fas trafficking from the lipid rafts portion to the non-lipid rafts portion, which was a time-dependent process. Beas-2B cells were exposed to RA or hyperoxia conditions. Lipid rafts were isolated as described under Materials and methods. Western blot analysis was used to detect Fas and Cav-1. (E) The deletion of Cav-1 prevented the formation of the Fas multimer after hyperoxia. Primary wild-type mouse lung epithelial cells (Cav-$1^{+/+}$) versus cells isolated from Cav-$1^{-/-}$ mice were used, and Fas multimerization was determined as described previously. (F) The deletion of Cav-1 caused the Fas expression to be up-regulated in both the absence and the presence of hyperoxia. Primary mouse lung epithelial cells were isolated, and cells were exposed to RA or hyperoxia (24 h). The protein level of Fas was determined by using Western blot analysis. For each panel, three independent assays are represented. $^{*}P<0.05$, $^{\#}P<0.01$.

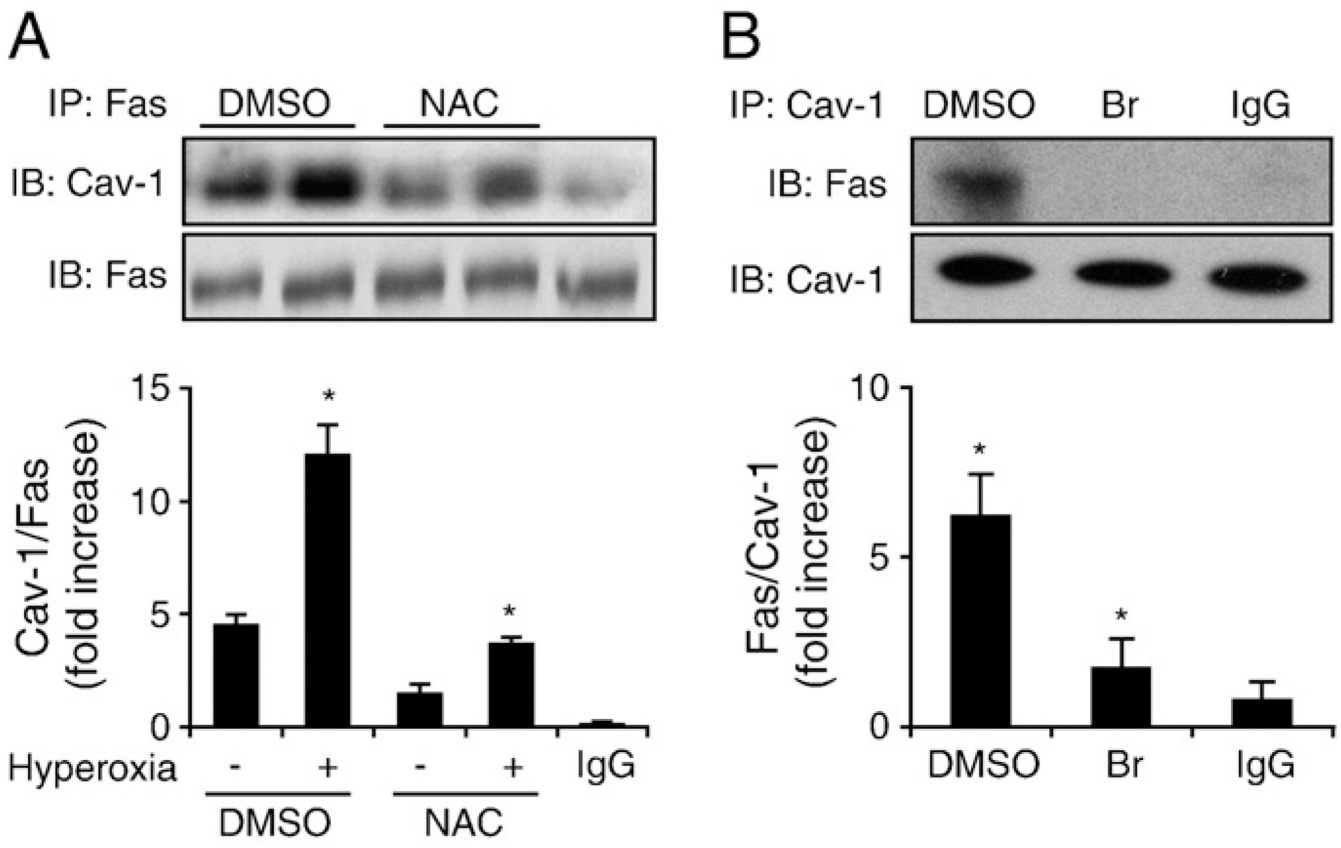

Fig. 4.

Cav-1 interacts with Fas after hyperoxia, partially *via* ROS and palmitoylation. (A) Blocking ROS with NAC (30 nM) partially eliminated Cav-1–Fas interaction. Beas-2B cells were pretreated with an NAC or PBS control, and then after 30 min, the cells were exposed to hyperoxia (4 h). Cell lysates were then collected, and co-IP assays were performed to determine Cav-1–Fas interactions. (B) Cav-1–Fas interaction after hyperoxia is mediated by palmitoylation. Beas-2B cells were pretreated with 2-Br (1 μM), and then after 30 min, the cells were exposed to hyperoxia (4 h). The Cav-1–Fas interaction was determined by using co-IP assays, as described previously. All blots represent three repeats. *P<0.05.

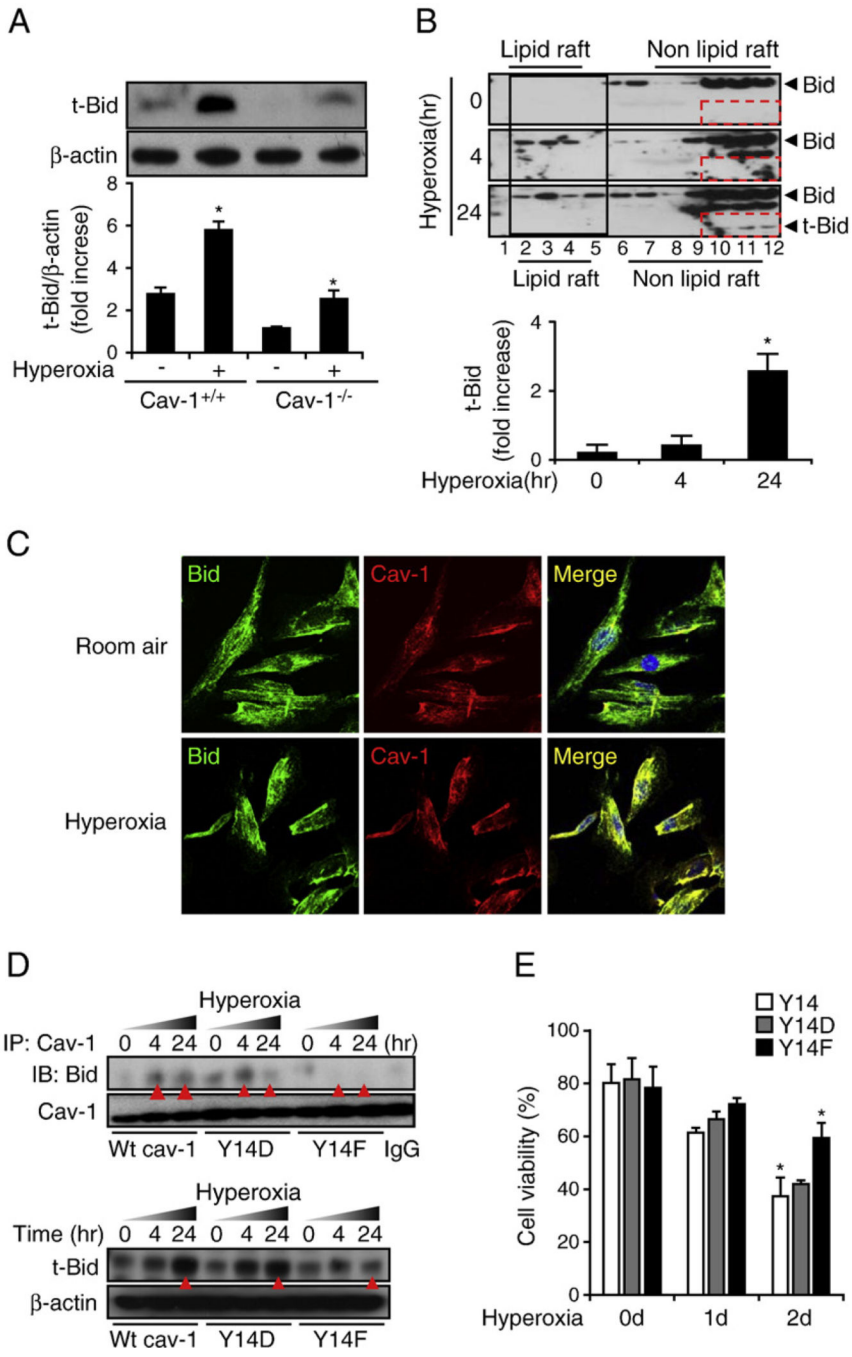

Fig. 5.

Cav-1 interacts with BID and regulates the hyperoxia-induced intrinsic and extrinsic apoptotic pathways. Primary mouse lung epithelial cells and Beas-2B human bronchial epithelial cells were used in this study. (A) The deletion of Cav-1 prevented the formation of truncated BID. Primary wild-type mouse lung epithelial cells (Cav-$1^{+/+}$) versus cells isolated from Cav-$1^{-/-}$ mice were used. Cells were exposed to hyperoxia (24 h), and the tBID level was detected. (B) Hyperoxia induced BID trafficking and tBID formation in Beas-2B cells. The lipid raft was isolated, as described previously. BID was then determined by using

Western blot analysis. Using goat polyclonal anti-BID (Santa Cruz Biotechnology), both the 22- and the 15-kDa segments may be detected. Hyperoxia induced BID trafficking from the nonlipid portion to the lipid portion of the rafts. (C) The colocalization between Cav-1 and BID in the absence or presence of hyperoxia (4 h). Beas-2B cells were stained with anti-Cav-1, anti-BID, and DAPI. The merged images are shown (right), representing the colocalization of Cav-1 and BID in the presence and absence of hyperoxia. (D) The mutation of Cav-1 phosphorylated tyrosine Y14 to Y14F disrupted the interaction between Cav-1 and BID. Two mutated clones (Y14F and Y14D), in addition to the wild-type Y14, were transfected into Beas-2B cells. The cells were then exposed to hyperoxia for 4 or 24 h. The Cav-1–BID interaction was determined by using co-IP assays. The tBID level was determined by using Western blot analysis. (E) Beas-2B cells that were transfected with Cav-1 Y14F, but not the wild-type Y14 or Y14D, show cytoprotective effects against hyperoxia-induced cell death. As described previously, after transfection with Y14, Y14D, or Y14F, Beas-2B cells were exposed to hyperoxia. After a designated time-frame, cell viability was determined as described under Materials and methods. All the above experiments represent a minimum of three repeats. *$P<0.05$.

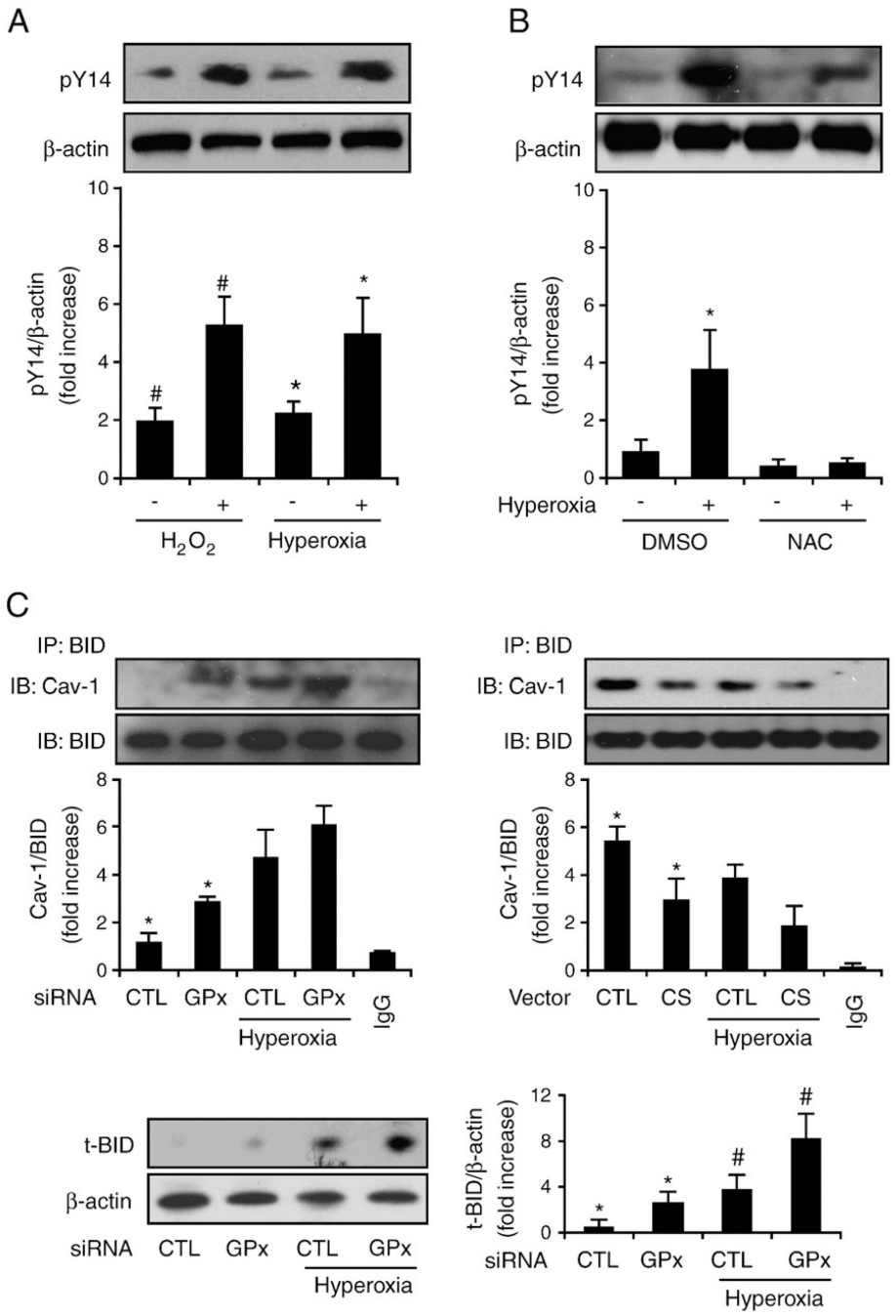

Fig. 6.

Hyperoxia induces Cav-1 phosphorylation *via* ROS. Beas-2B human bronchial epithelial cells and primary mouse lung epithelial cells were used in these experiments. (A) Hyperoxia and H_2O_2 induce Cav-1 phosphorylation. Primary lung epithelial cells derived from C57BL/6 mice were incubated with 90 μM H_2O_2 for 20 min, exposed to hyperoxia (4 h), or left untreated. Cell lysates were collected and analyzed by Western blotting and were blotted with anti-PY14Cav-1. (B) NAC blocks hyperoxia-induced Cav-1 Y14 phosphorylation. Primary lung epithelial cells were pretreated with NAC (30 nM), which was followed by

exposure to hyperoxia (4 h). Western blot analysis was used to determine Y14 phosphorylation. Similar results were found in Beas-2B cells. (C) Beas-2B cells were transfected with GPX2 siRNA or control siRNA (left) or with catalase overexpression clones or control vectors (right). After 24 h, cells were exposed to hyperoxia (4 h). Coimmunoprecipitation of Cav-1 and BID was determined. Cell lysates were incubated with anti-BID antibody overnight at 4 °C and then coupled with protein A/G agarose beads. The Cav-1 protein, which coimmunoprecipitated with BID, was detected by Western blotting. Incubation of the same amount of lysate with rabbit IgG was used as a negative control. A representative of at least three experiments is shown. IP, immunoprecipitation; IB, immunoblot. (C, bottom) Cells transfected with GPX2 siRNA have elevated tBID. Beas-2B cells were transfected with GPX2 siRNA or control siRNA as above. tBID was determined by Western blot analysis. $^{*}P<0.05$, $^{\#}P<0.05$.

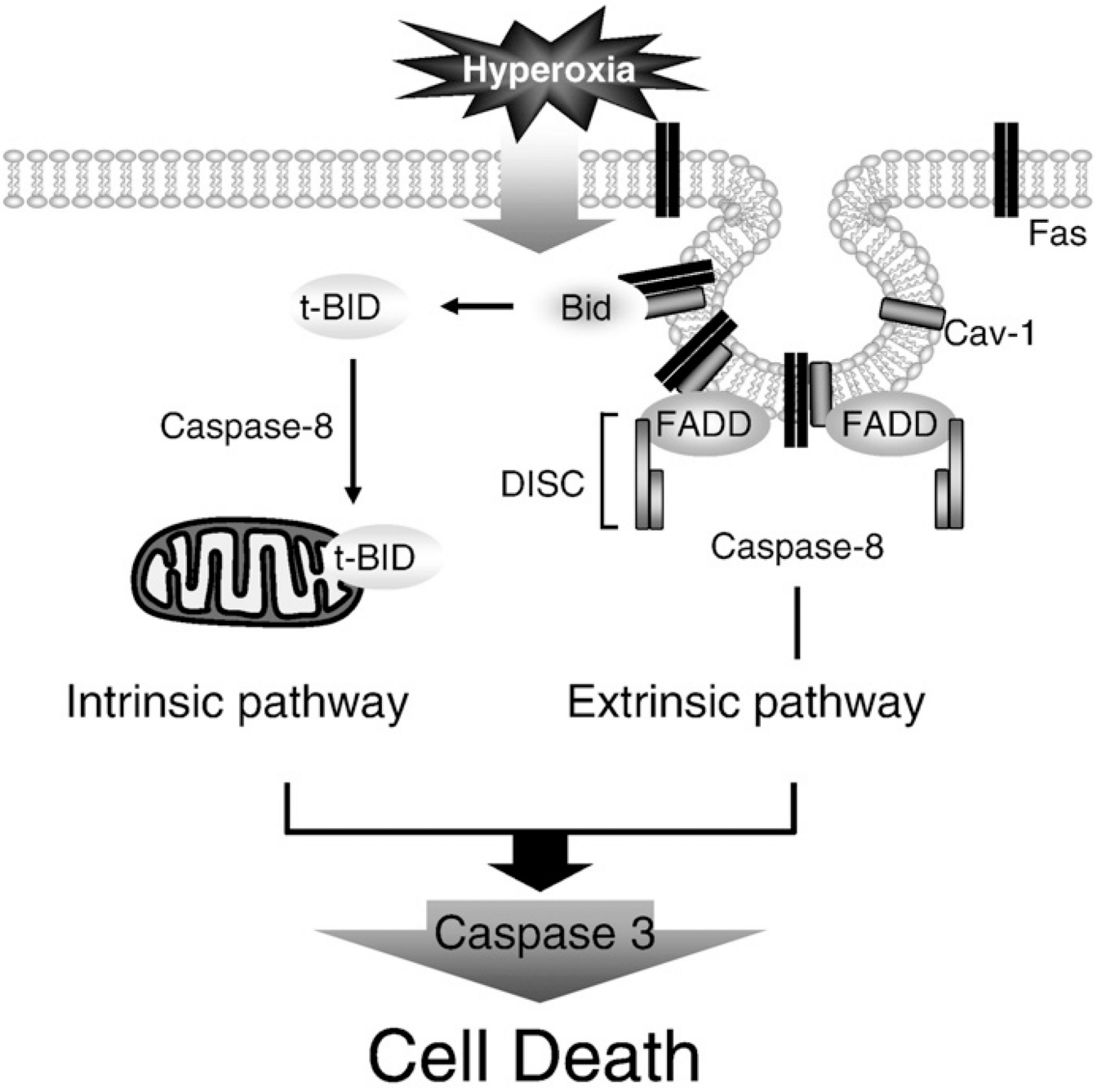

Fig. 7.

Schematic illustration of the mechanisms by which Cav-1 regulates hyperoxia-induced extrinsic and intrinsic apoptotic pathways in lung epithelial cells. Hyperoxia induces Fas/Cav-1 palmitoylation and hence induces Fas–Cav-1 interaction. By interacting with Fas, Cav-1 facilitates Fas multimerization and initiates DISC formation, which subsequently activates caspase 8. Meanwhile, hyperoxia induces Cav-1 Y14 phosphorylation, which then induces Cav-1–BID interaction. The interaction between Cav-1 and BID *via* Y14 phosphorylation increases the proximity of BID to activated caspase 8. Therefore, Cav-1

also facilitates the truncation of BID to tBID by caspase 8. tBID translocates to the mitochondria and mediates the release of mitochondrial cytochrome *c*, which induces intrinsic apoptotic pathways, resulting in elevated caspase 9 activity.